1 January 2002

Optics Communications 201 (2002) 105–112

OPTICS COMMUNICATIONS

www.elsevier.com/locate/optcom

Quantum anticorrelation between orthogonal-polarization modes of laser diode at cryogenic temperature

Ruifang Dong [a,*], Junxiang Zhang [a], Tiancai Zhang [b], Changde Xie [a]

[a] *The Key Laboratory of Quantum, Optics, Ministry of Education, PR China*

[b] *Institute of Opto-Electronics, Shanxi University, Taiyuan, Shanxi 030006, PR China*

Received 20 April 2001; accepted 9 October 2001

Abstract

The anticorrelation between quantum fluctuations of two orthogonal-polarization modes resulting from the strain-induced birefringence in laser medium of laser diode is calculated and analyzed based on considering the common carrier population coupling and gain fluctuation correlation between the two modes. The numerical calculation results can account for the polarization dependence of LD intensity noise phenomenally and present us an image of the anticorrelation behavior in the LD at low temperature. © 2002 Published by Elsevier Science B.V.

PACS: 42.50.Dv

1. Introduction

As well known, laser diodes (LDs) operating at cryogenic temperature have favorite features such as lower threshold, higher quantum efficiency and lower quantum noise [1–4]. The photon-number squeezed light with the photon-number fluctuation below the Shot-Noise-Limit (SNL) has been generated from various LD systems by means of line narrowing techniques [4–6] and has been applied on measurements with precision beyond the SNL [7–10]. While the experimental measurements for amplitude fluctuation spectra from the nonclassical output of an injection-locked low-temperature quantum-well laser revealed polarization-dependence of the photon-number statistics of the output laser field [11–13], a thorough understanding of the noise behavior in such lasers has great importance in fields from optical communication to high-sensitivity spectroscopy. The observed polarization-dependent noise were accounted qualitatively in [12] for polarization mixed by strain-induced birefringent components and correlated fluctuations of the two orthogonal-polarization lasing modes in the laser gain medium, the latter stems from mode competition that is due to the homogeneous part of the gain spectrum [14–20]. A detailed theoretical calculation

* Corresponding author. Fax: +86-351-701-1500.
E-mail address: dong_ruif@263.net (R. Dong).

0030-4018/02/$ - see front matter
PII: S0030-4018(01)01620-0

on the anticorrelation between the two polarization modes has been presented in our paper. Since the two modes lase at the same frequency, unlike the case in a VCSEL [16–20], the correlations are between field amplitudes, whose physical origin are related to the correlation of the gain fluctuations of them.

In this paper, the quantum anticorrelation between parallel and perpendicularly polarized modes relative to strain-induced birefringent axis formed inside the laser cavity in a cryostat is calculated with the operator Langevin equations that is similar to the method employed in the successful discussions to the quantum correlation between longitudinal-mode intensities in a multimode LD laser [14]. Tracing back to the physical origin of linear-polarization operation, the intracavity losses of the laser mode parallel polarized to the emitting junction (TE mode) of LD are far lower than that of the mode perpendicularly polarized to the junction (TM mode), so that the output of the TM mode tends to zero due to the mode-competition effect of cavity and we assume reasonably that a line-narrowed LD emits single-mode laser of pure linear polarization along the laser emitting junction in the cavity at room temperature. At low temperature the laser medium of LD presents anisotropic feature owing to the strain-induced birefringence. Thus the output light of laser is elliptically polarized, θ represents the orientation of the ellipse relative to the emitting junction. When θ becomes larger, the projection of the elliptical polarized light onto the laser emitting junction will reduce, and meanwhile the projection onto the perpendicular axis of the junction will increase. In this case, it seems that the decay rate of the mode parallel to the laser junction becomes larger, and the decay rate of the other mode being perpendicular to the laser junction becomes smaller. So we suppose in our calculation that the ratio of decay rate of the light with different polarization orientation in laser cavity gradually increases when the angle of the polarization θ relative to the emitting junction becomes larger. In our theoretical model the laser medium is processed as an uniaxial-like material in which only two orthogonal-polarization modes with same frequency are permitted, one is parallel to the birefringent axis (M_1 mode) and the other one is perpendicular (M_2 mode). Usually the strain-induced birefringence is weak, thus the angle θ between the birefringent axis and laser emitting junction is far smaller than 45°, the decay rate of M_1 mode is much smaller than that of M_2 mode. The stronger the birefringence, the larger the angle θ. Without birefringence ($\theta = 0$), pure linear-polarized laser (TE mode) is transmitted. With birefringence ($\theta \neq 0$), since M_1 and M_2 modes are coupled to a common carrier population, there are anticorrelated quantum fluctuations between them which are similar to the analysis in [14–20]; At the same time, M_1 and M_2 modes simultaneously resonate with same frequency and different transmitting velocities in the laser medium, the stimulated-emission-gain fluctuation operators of M_1 and M_2 modes are quantum anticorrelated and the total output field becomes ellipticaly polarized.

With $1/\tau_{p1}$ and $1/\tau_{p2}$ standing for the intracavity decay rate of M_1 and M_2 modes, respectively, the parameter $k = \tau_{p2}/\tau_{p1}$ is evaluated from 0 to 1 when the angle θ varies from 0 to 45° relative to different birefringence. We numerically calculated the correlation factor between M_1 and M_2 mode, the amplitude noise spectral densities of the output M_1, M_2 modes and the composed mode of M_1 and M_2 noise spectra. Based on the published experimental data [12], the calculated anticorrelation resulting from birefringent laser medium is equal to -0.54 at 40 MHz, which is less than the value of -0.7 measured by the experiment in [12]. In the experiment, a collimating lens is also placed in the cryostat and the strain-induced birefringence of the lens at low-temperature generates behavior that is qualitatively similar to anticorrelated photon-number fluctuation [12]. If the anticorrelation resulting from the external optical element is appropriately considered the total correlation should be closer to the experimental measurement.

2. Amplitude fluctuating spectral densities and quantum anticorrelation of intracavity modes and output fields

When there is a strain-induced birefringence in the laser medium at low temperature, two orthogonal-polarized modes parallel and perpendicular to the birefringent axis M_1 and M_2 simultaneously resonate in the cavity and the quantum fluctuation of photon numbers of the two modes are anticorrelated due to the common carrier population coupling [14]. To simplify analysis, we assume:

(a) there are only two modes M_1 and M_2 in the resonator;
(b) the output coupling losses of the two modes are equal;
(c) carrier population inversion is ideal;
(d) the pumping noise is completely suppressed.

The Quantum-mechanic Langevin equations for the photon-number operators $\widehat{n}_1$ and $\widehat{n}_2$ of the two modes M_1 and M_2, and the carrier population operator $\tilde{N}_c$ can be given as follows:

$$\frac{d(\widehat{n}_1+\widehat{n}_2)}{dt} = -\frac{1}{\tau_1}\widehat{n}_1 - \frac{1}{\tau_2}\widehat{n}_2 + \tilde{A}(t)(\widehat{n}_1+\widehat{n}_2+1) + \tilde{G}_1(t) + \tilde{G}_2(t) + \widehat{g}_1(t) + \widehat{g}_2(t) + \widehat{f}_1(t) + \widehat{f}_2(t), \quad (2.1)$$

$$\frac{d\tilde{N}_c}{dt} = p - \frac{\tilde{N}_c}{\tau_{sp}} - \tilde{A}(t)(\widehat{n}_1+\widehat{n}_2+1) + \tilde{\Gamma}_p(t) + \tilde{\Gamma}_{sp}(t) + \tilde{\Gamma}(t), \quad (2.2)$$

where the subscript '1' stands for M_1 mode, the subscript '2' for M_2 mode, $1/\tau_i$ $(i = 1,2)$ represents the photon-number decay rate of the modes, which is the sum of the internal loss $1/\tau_{pi}$ and the output coupling loss $1/\tau_{pe}$,

$$\frac{1}{\tau_i} = \frac{1}{\tau_{pi}} + \frac{1}{\tau_{pe}}. \quad (2.3)$$

$\tilde{A}(t)$ denotes the spontaneous-emission rate,

$$\tilde{A}(t) = \frac{\beta\tilde{N}_c}{\tau_{sp}}, \quad (2.4)$$

where β and τ_{sp} are the spontaneous-emission coefficient and the spontaneous-emission lifetime of the carriers in the laser medium.

Under the condition of ideal carrier population inversion, the stimulated absorption rate $\tilde{E}_{vc}$ can be neglected, and from Einstein's relationship, we get

$$\tilde{A}(t) = \tilde{E}_{cv}. \quad (2.5)$$

$\tilde{E}_{cv}$ is the stimulated-emission rate of the electrons. The noise operators $\tilde{G}_i(t)$, $\widehat{g}_i(t)$ and $\widehat{f}_i(t)$ are associated with the random processes of stimulated-emission gain, internal loss and output coupling loss. The correlation fluctuations of these noise operators are [14]

$$\langle\tilde{G}_i(t)\tilde{G}_i(u)\rangle = \delta(t-u)\langle\widehat{E}_{cv}\rangle\langle\widehat{n}_i\rangle, \quad (2.6)$$

$$\langle\widehat{g}_i(t)\widehat{g}_i(u)\rangle = \delta(t-u)\frac{1}{\tau_{pi}}\langle\widehat{n}_i\rangle, \quad (2.7)$$

$$\langle\widehat{f}_i(t)\widehat{f}_i(u)\rangle = \delta(t-u)\frac{1}{\tau_{pe}}\langle\widehat{n}_i\rangle. \quad (2.8)$$

In Eq. (2.2), p is the pumping rate, $\tilde{\Gamma}_p(t)$, $\tilde{\Gamma}_{sp}(t)$ and $\tilde{\Gamma}(t)$ stand for the pumping noise, the spontaneous-emission noise and the stimulated-emission noise, respectively. The correlation functions of these noise operators are [14]

$$\langle\tilde{\Gamma}_p(t)\tilde{\Gamma}_p(u)\rangle = 0, \quad (2.9)$$

$$\langle\tilde{\Gamma}_{sp}(t)\tilde{\Gamma}_{sp}(u)\rangle = \delta(t-u)\frac{\langle\tilde{N}_c\rangle}{\tau_{sp}}, \quad (2.10)$$

$$\langle\tilde{\Gamma}(t)\tilde{\Gamma}(t)\rangle = \delta(t-u)\langle\widehat{E}_{\mathrm{cv}}\rangle(\langle\widehat{n}_1\rangle + \langle\widehat{n}_2\rangle). \tag{2.11}$$

Since the two operators $\tilde{G}_i(t)$ and $\tilde{\Gamma}(t)$ come from the same origin (the stimulated-emission processes), they have the correlation

$$\langle\tilde{G}_i(t)\tilde{\Gamma}(t)\rangle = -\delta(t-u)\langle\widehat{E}_{\mathrm{cv}}\rangle\langle\widehat{n}_i\rangle. \tag{2.12}$$

2.1. Amplitude fluctuating spectral densities of intracavity M_1 and M_2 modes

As the laser oscillates above the threshold, the quasilinearization procedure is available:

$$\tilde{N}_{\mathrm{c}}(t) = \langle\tilde{N}_{\mathrm{c}}\rangle + \Delta\tilde{N}_{\mathrm{c}}(t) = N_{\mathrm{c}0} + \Delta\tilde{N}_{\mathrm{c}}(t), \tag{2.13}$$

$$\widehat{n}_i(t) = \langle\widehat{n}_i\rangle + \Delta\widehat{n}_i = a_{i0}^2 + 2a_{i0}\Delta\widehat{a}_i(t), \tag{2.14}$$

$$\tilde{A}(t) = \langle\tilde{A}\rangle + \frac{\mathrm{d}\langle\tilde{A}\rangle}{\mathrm{d}N_{\mathrm{c}0}}\Delta\tilde{N}_{\mathrm{c}}(t) = \frac{\beta N_{\mathrm{c}0}}{\tau_{\mathrm{sp}}} + \frac{\beta}{\tau_{\mathrm{sp}}}\Delta\tilde{N}_{\mathrm{c}}(t), \tag{2.15}$$

where a_{i0}^2 and $\Delta\widehat{a}_i(t)$ are the average amplitude and the amplitude fluctuation operator, $N_{\mathrm{c}0}$ is the mean carrier population and $\Delta\tilde{N}_{\mathrm{c}}(t)$ is the fluctuation operator of the carrier population.

According to the quasilinear treatment, we get the equations for the fluctuating operators:

$$\frac{\mathrm{d}\Delta\widehat{a}_1}{\mathrm{d}t} = A_{11}\Delta\widehat{a}_1 + A_{21}\Delta\tilde{N}_{\mathrm{c}} + \frac{1}{2a_{10}}(\tilde{G}_1(t) + \widehat{g}_1(t) + \widehat{f}_1(t)), \tag{2.16}$$

$$\frac{\mathrm{d}\Delta\widehat{a}_2}{\mathrm{d}t} = A_{12}\Delta\widehat{a}_2 + A_{22}\Delta\tilde{N}_{\mathrm{c}} + \frac{1}{2a_{20}}(\tilde{G}_2(t) + \widehat{g}_2(t) + \widehat{f}_2(t)), \tag{2.17}$$

$$\frac{\mathrm{d}\Delta\tilde{N}_{\mathrm{c}}}{\mathrm{d}t} = A_3\Delta\tilde{N}_{\mathrm{c}} + A_4\Delta\widehat{a}_1 + A_5\Delta\widehat{a}_2 + \tilde{\Gamma}_{\mathrm{p}}(t) + \tilde{\Gamma}_{\mathrm{sp}}(t) + \tilde{\Gamma}(t). \tag{2.18}$$

Performing the Fourier transformation to Eqs. (2.16)–(2.18) under the limit of the analyzing frequency $\Omega \to 0$, we obtain the expression for the amplitude fluctuation operator $\Delta\widehat{a}_i(0)$ of M_1 and M_2 modes

$$\Delta\widehat{a}_1(0) = R \times \{A_{12}A_{21}\tilde{F}(0) - (A_3A_{12} - A_5A_{22})\widehat{H}_{r1}(0) - A_5A_{21}\widehat{H}_{r2}(0)\}, \tag{2.19}$$

$$\Delta\widehat{a}_2(0) = R \times \{A_{11}A_{22}\tilde{F}(0) - (A_3A_{11} - A_4A_{21})\widehat{H}_{r1}(0) - A_4A_{22}\widehat{H}_{r2}(0)\}, \tag{2.20}$$

where

$$A_{11} = \frac{\beta N_{\mathrm{c}0}}{\tau_{\mathrm{sp}}} - \frac{1}{\tau_1}, \quad A_{12} = \frac{\beta N_{\mathrm{c}0}}{\tau_{\mathrm{sp}}} - \frac{1}{\tau_2}, \quad A_{21} = \frac{\beta a_{10}}{2\tau_{\mathrm{sp}}}, \quad A_{22} = \frac{\beta a_{20}}{2\tau_{\mathrm{sp}}},$$

$$A_3 = -\left(\frac{1}{\tau_{\mathrm{sp}}} + \frac{\beta a_{10}^2}{\tau_{\mathrm{sp}}} + \frac{\beta a_{20}^2}{\tau_{\mathrm{sp}}}\right), \quad A_4 = -2a_{10} \times \frac{\beta N_{\mathrm{c}0}}{\tau_{\mathrm{sp}}}, \quad A_5 = -2a_{20} \times \frac{\beta N_{\mathrm{c}0}}{\tau_{\mathrm{sp}}},$$

$$R = (A_3A_{11}A_{12} - A_4A_{12}A_{21} - A_5A_{11}A_{22})^{-1},$$

$$\widehat{H}_{\mathrm{ri}}(0) = \frac{1}{2a_{10}}(\tilde{G}_i(0) + \widehat{g}_i(0) + \widehat{f}_i(0)), \quad \tilde{F}(0) = \widehat{\Gamma}_{\mathrm{p}}(0) + \widehat{\Gamma}_{\mathrm{sp}}(0) + \widehat{\Gamma}(0).$$

2.2. Amplitude fluctuating spectral densities of the output fields

The amplitude fluctuating operator $\Delta\widehat{r}_i(t)$ of the output laser mode is composed of the internal field fluctuation and the injected external zero-point fluctuation

$$\Delta\widehat{r}_i(t) = \left(\frac{1}{\tau_{\rm pe}}\right)^{1/2}\Delta\widehat{a}_i(t) - \widehat{e}_i(t). \tag{2.21}$$

The correlation function of the external zero-point fluctuation operator $\widehat{e}_i(t)$ is expressed as

$$\langle\widehat{e}_i(t)\widehat{e}_i(u)\rangle = \delta(t-u)\tfrac{1}{2}. \tag{2.22}$$

Since the fluctuating operator $\widehat{f}_i(t)$ denotes the contribution of the zero-point fluctuation $\widehat{e}_i(t)$ injected from the output coupler, the correlation between $\widehat{e}_i(t)$ and $\widehat{f}_i(t)$ is

$$\langle\widehat{e}_i(t)\widehat{f}_i(t)\rangle = \delta(t-u)\frac{a_{i0}}{2\sqrt{\tau_{\rm pe}}}. \tag{2.23}$$

Because of the birefringence in the laser medium at low temperature, M_1 and M_2 modes simultaneously resonate and lase at the same frequency, the stimulated-emission-gain fluctuation operators of M_1 and M_2 modes $\tilde{G}_1(t)$, $\tilde{G}_2(t)$ come from the same origin and correlate each other

$$\langle\tilde{G}_1(t)\tilde{G}_2(u)\rangle = -\delta(t-u)\langle\widehat{E}_{\rm cv}\rangle\sqrt{\langle\widehat{n}_1\rangle\langle\widehat{n}_2\rangle} = -\delta(t-u)\frac{\beta N_{\rm c0}}{\tau_{\rm sp}}a_{10}a_{20}. \tag{2.24}$$

Substituting (2.19) and (2.20) into the Fourier transformation of (2.21), we obtain the expressions for the fluctuating spectral densities of the output components of M_1, M_2 modes, and cross-correlation between M_1 and M_2 at $\Omega \to 0$.

$$\begin{aligned} P_{\Delta\widehat{r}_1}(0) = {} & \tfrac{1}{2} + 2(A_3A_{12} - A_5A_{22})D_1 + A_{12}^2A_{21}^2D_2 + (A_3A_{12} - A_5A_{22})^2D_4 - A_5A_{12}A_{21}^2D_5 \\ & - (A_3A_{12}^2A_{21} - A_5A_{12}A_{21}A_{22})D_3 + (A_3A_5A_{21}A_{12} - A_5^2A_{22}A_{21})D_6 + A_5^2A_{21}^2D_7, \end{aligned} \tag{2.25}$$

$$\begin{aligned} P_{\Delta\widehat{r}_2}(0) = {} & \tfrac{1}{2} + 2(A_3A_{11} - A_4A_{21})D_1 + A_{11}^2A_{21}^2D_2 - A_4A_{11}A_{22}^2D_3 + A_4^2A_{22}^2D_4 \\ & - (A_3A_{11}^2A_{22} - A_4A_{11}A_{21}A_{22})D_5 + (A_3A_4A_{11}A_{21} - A_4^2A_{22}A_{21})D_6 + (A_3A_{11} - A_4A_{21})^2D_7, \end{aligned} \tag{2.26}$$

$$\begin{aligned} \langle\Delta\widehat{r}_1(0)\Delta\widehat{r}_2(0)\rangle = {} & (A_4A_{22} + A_5A_{21})D_1 + A_{11}A_{12}A_{21}A_{22}D_2 \\ & - \tfrac{1}{2}(A_3A_{11}A_{12}A_{22} + A_4A_{12}A_{21}A_{22} - A_5A_{11}A_{22}^2)D_3 \\ & - (A_3A_{11}A_{12}A_{21} - A_4A_{12}A_{21}^2 + A_5A_{11}A_{21}A_{22})D_5 \\ & + \tfrac{1}{2}(A_3^2A_{11}A_{12} - A_3A_4A_{12}A_{21} - A_3A_5A_{11}A_{22} + 2A_4A_5A_{21}A_{22})D_6 \\ & + (A_3A_4A_{12}A_{22} - A_4A_5A_{22}^2)D_4 + (A_3A_5A_{11}A_{21} - A_4A_5A_{21}^2)D_7. \end{aligned} \tag{2.27}$$

Then at a certain analyzing frequency Ω, the fluctuating spectral densities of the output components of M_1, M_2 modes, and the total field, and cross-correlation between M_1 and M_2 can be written as

$$P_{\Delta\widehat{r}_1}(\Omega) = \frac{P_{\Delta\widehat{r}_1}(0)}{1 + \left(\frac{\Omega}{A_{11}}\right)^2} + \frac{\Omega^2}{A_{11}^2 + \Omega^2} \times \frac{1}{2}, \tag{2.28}$$

$$P_{\Delta\widehat{r}_2}(\Omega) = \frac{P_{\Delta\widehat{r}_1}(0)}{1 + \left(\frac{\Omega}{A_{12}}\right)^2} + \frac{\Omega^2}{A_{12}^2 + \Omega^2} \times \frac{1}{2}, \tag{2.29}$$

$$\langle \Delta\widehat{r}_1(\Omega)\Delta\widehat{r}_2(\Omega)\rangle = \frac{A_{11}A_{12}(A_{11}A_{12}+\Omega^2)}{(A_{11}A_{12}+\Omega^2)^2+\Omega^2(A_{11}-A_{12})^2}\langle \Delta\widehat{r}_1(0)\Delta\widehat{r}_2(0)\rangle, \tag{2.30}$$

$$C_1(\Omega) = \frac{\frac{A_{11}A_{12}(A_{11}A_{12}+\Omega^2)}{(A_{11}A_{12}+\Omega^2)^2+\Omega^2(A_{11}-A_{12})^2}\langle \Delta\widehat{r}_1(0)\Delta\widehat{r}_2(0)\rangle}{\sqrt{\left(\frac{P_{\widehat{\Delta r_1}}(0)}{1+\left(\frac{\Omega}{A_{11}}\right)^2}+\frac{\Omega^2}{A_{11}^2+\Omega^2}\times\frac{1}{2}\right)\left(\frac{P_{\widehat{\Delta r_1}}(0)}{1+\left(\frac{\Omega}{A_{12}}\right)^2}+\frac{\Omega^2}{A_{12}^2+\Omega^2}\times\frac{1}{2}\right)}}, \tag{2.31}$$

$$P_{\widehat{\Delta r_1}}(\Omega) = \left(P_{\widehat{\Delta r_1}}(\Omega)n_{10}+P_{\widehat{\Delta r_2}}(\Omega)n_{20}+2\langle \Delta\widehat{r}_1(\Omega)\Delta\widehat{r}_2(\Omega)\rangle\sqrt{n_{10}n_{20}}\right)\Big/(n_{10}+n_{20}), \tag{2.32}$$

where

$$D_1 = R\times\frac{1}{4\tau_{\text{pe}}},\quad D_2 = R^2\times\frac{\left(p-\frac{\beta N_{c0}}{\tau_{\text{sp}}}\right)}{\tau_{\text{pe}}},\quad D_3 = R^2\times\frac{\left(-a_{10}\frac{\beta N_{c0}}{\tau_{\text{sp}}}\right)}{\tau_{\text{pe}}},\quad D_4 = R^2\times\frac{\left(\frac{1}{\tau_1}+\frac{\beta N_{c0}}{\tau_{\text{sp}}}\right)}{4\tau_{\text{pe}}},$$

$$D_5 = R^2\times\frac{\left(-a_{20}\frac{\beta N_{c0}}{\tau_{\text{sp}}}\right)}{\tau_{\text{pe}}},\quad D_6 = -R^2\times\frac{\frac{\beta N_{c0}}{\tau_{\text{sp}}}}{2\tau_{\text{pe}}},\quad D_7 = R^2\times\frac{\left(\frac{1}{\tau_2}+\frac{\beta N_{c0}}{\tau_{\text{sp}}}\right)}{4\tau_{\text{pe}}}.$$

3. Numerical results analysis

In the calculation of anticorrelation produced by the birefringence of laser diode, if neglecting the fluctuating terms in a Langevin equations (2.1) and (2.2), we get the steady-state equations. The mean carrier population N_{c0} and the mean photon numbers n_{10} and n_{20} of M_1 and M_2 modes satisfy the following equations:

$$\left(\frac{\beta N_{c0}}{\tau_{\text{sp}}}-\frac{1}{\tau_1}\right)n_{10}+\left(\frac{\beta N_{c0}}{\tau_{\text{sp}}}-\frac{1}{\tau_2}\right)n_{20} = \frac{\beta N_{c0}}{\tau_{\text{sp}}}, \tag{3.1}$$

$$\frac{\beta N_{c0}}{\tau_{\text{sp}}}(n_{10}+n_{20}+1)+\frac{N_{c0}}{\tau_{\text{sp}}} = p, \tag{3.2}$$

$$n_{10}+n_{20} = R/\beta, \tag{3.3}$$

where R is the normalized pumping rate, $R = (p/p_{\text{th}})-1$, p_{th} is the pumping threshold. Solving the steady-state equations (3.1)–(3.3), the analytic expressions for N_{c0}, n_{10} and n_{20} were obtained. We numerically analyze the fluctuating spectral densities of the output M_1, M_2 modes and the total field, and the cross-correlation between M_1 and M_2 mode at $\Omega = 40$ MHz as the functions of the parameter $k = \tau_{p2}/\tau_{p1}$. From Fig. 2 in [12], the amplitude fluctuations of the output elliptically polarized components along the long and short axes of the ellipse at 40 MHz are -1 and 12.4 dB, respectively, and the intensity ratio between them measured by the experiment is 170:1, while the amplitude fluctuation of the total output field at 40 MHz is -2.6 dB. Taking $R = 20$, $p_{\text{th}} = 1.6\times10^{16}$, $\tau_{\text{sp}} = 3\times10^{-9}$ s, $\beta = 1\times10^{-4}$, $\tau_{\text{pe}} = 1.11\times10^{-12}$ s, $\tau_{p1} = 1.434\times10^{-12}$ s, the best matching between the calculation and the experiment is reached. Substituting

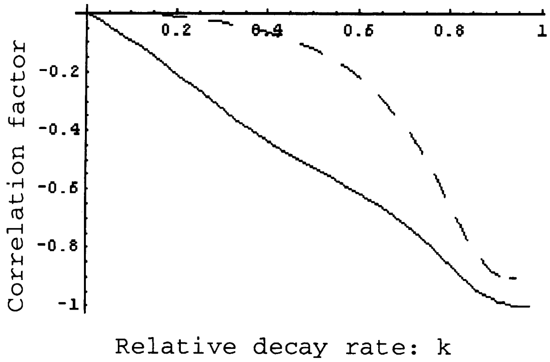

Fig. 1. The cross-correlation spectral densities between the two output fields of M_1 and M_2 modes from the LD at Ω 40 MHz as a function of the relative decay rate parameter k. The dashed line is the calculated correlation in which the stimulated-emission-gain fluctuation is not included and the solid line is the calculated result in which both anticorrelations resulting from the photon-number fluctuation and the stimulated-emission-gain fluctuation are calculated.

these values into Eqs. (2.28)–(2.32), the function curves of the cross-correlation spectral densities and the fluctuating spectral densities of the output fields from the laser diode versus k from 0 to 1 were obtained (Figs. 1 and 2). We see from Fig. 2 that when $k = 0.526$, the amplitude fluctuation of the total output field is -2.66 dB, the amplitude fluctuations of the output M_1 and M_2 modes are -1.53 and 12.42 dB, respectively. In the calculation the intensity ratio of M_1 mode to M_2 mode is taken as 323:1 since in fact the birefringence in the collimating lens at low temperature will reduce the ratio at some extent, therefore the ratio induced by the birefringence of the laser medium should be larger than the measured value 170:1 outside the cryostat. The cross-correlation between M_1 and M_2 mode at $k = 0.526$ is $C_1 = -0.54$ as shown in Fig. 1. It is smaller than the experimental value −0.7 measured outside the cryostat, that is because the birefringent effect of the collimating lens in not considered.

In contrast with the anticorrelation effects between the amplitude fluctuations of M_1 and M_2 modes, the anticorrelation effects between the intensity fluctuations of two modes [14–20] are also analyzed. In Fig. 1 the solid line is the calculated correlation in the former condition, and the dashed line is the calculated result of the latter. We can see that if the correlation of the stimulated-emission-gain fluctuation operators of M_1 and M_2 modes (Eq. (2.24)) is not taken into account in the calculation, only the anticorrelation of the intensity fluctuations is involved [12,13], the calculated correlation with the same parameters is -0.14 instead of -0.54, which cannot explain the experimental results [12].

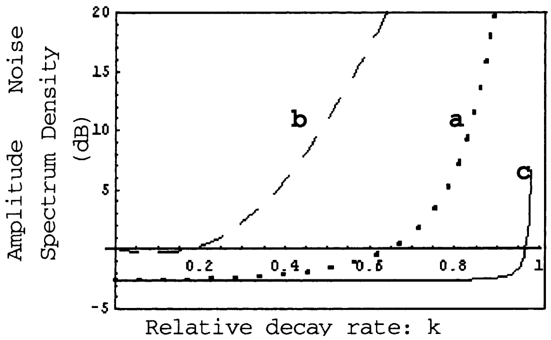

Fig. 2. The amplitude fluctuating spectral densities of the output fields from the LD at $\Omega = 40$ MHz as a function of k. The dotted line corresponds to that of M_1 mode, the dashed line to M_2 mode, and the solid line to the total light field.

4. Conclusion

We present a detailed theoretical analysis for the quantum anticorrelation between the two orthogonal-polarized modes in the laser medium of LD with the strain-induced birefringence at low temperature. The anticorrelation partially explains the experiment results that the intensity noise increases after the output light from LD in a cryostat passes through a polarizer [11–13]. If the influence of the external optical element at low temperature, such as the collimating lens, is taken into account, the totally calculated anticorrelation should be responsible for the experimental observation. We consider that the physical mechanisms of the anticorrelation resulting from laser medium and the external optics are totally different, the former is due to the real quantum processes of the common carrier coupling and gain fluctuation correlation, but the latter is only due to the polarization mixing to generate the behavior similar to the correlated photon-number fluctuation, in which there is no any quantum effect. The paper can provide us with a further understanding of the anticorrelation effects between the two modes with orthogonal polarizations on the noise of the semicondutor lasers at low temperature.

Acknowledgements

This research is supported by the National Natural Science Foundation of China (No. 69837010), the Oversea Youth Scholar Collaboration Foundation (No. 69928504) and the Shanxi Province Young Science Foundation (No. 20001016).

References

[1] S. Machida, Y. Yamamoto, Phys. Rev. Lett. 60 (1988) 792.
[2] W.H. Richardson, R.M. Shelby, Phys. Rev. Lett. 64 (1990) 400.
[3] W.H. Richardson, S. Machida, Y. Yamamoto, Phys. Rev. Lett. 66 (1991) 2867.
[4] S. Inoue, S. Machida, Y. Yamamoto, Phys. Rev. A 48 (1993) 2230.
[5] J. Kitching, R. Boyd, A. Yariv, Y. Shevy, Opt. Lett. 19 (1994) 1331.
[6] A. Furusawa, Opt. Lett. 21 (1996) 2014.
[7] W.H. Richardson, Y. Yamamoto, Phys. Rev. A 44 (1991) 7702.
[8] D.C. Kilper, A.C. Schaefer, J. Erland, D.G. Steel, Phys. Rev. A 54 (1996) 1785.
[9] Y.Q. Li, P. Lynam, M. Xiao, P.J. Edwards, Phys. Rev. Lett. 78 (1997) 3105.
[10] Y.Q. Li, M. Xiao, Opt. Express 2 (1998) 110.
[11] M.J. Freeman, H. Wang, D.G. Steel, R. Graig, D.R. Scifres, Opt. Lett. 18 (1993) 379; H. Wang, M.J. Freeman, D.G. Steel, Phys. Rev. Lett. 71 (1993) 3951.
[12] D.C. Kilper, D.G. Steel, R. Graig, D.R. Scofres, Opt. Lett. 21 (1996) 1283.
[13] D.C. Kilper, P.A. Roos, J.L. Carlsten, Phys. Rev. A 55 (1997) 3323.
[14] S. Inoue, H. Ohzu, S. Machida, Y. Yamamoto, Phys. Rev. A 46 (1992) 2757.
[15] F. Marin, B. Bramati, E. Giacobino, T.C. Zhang, J.-Ph. Poizat, J.-F. Roch, Ph. Grangier, Phys. Rev. Lett. 75 (1995) 4606.
[16] A.W. Smith, J.A. Armstrong, IBM Syst. J. 10 (1996) 225.
[17] F. Marin, G. Giacomelli, J. Opt. B 1 (1999) 128.
[18] A. Branati, J.-P. Hermier, A.Z. Khoury, E. Giacobino, P. Schnitzer, R. Michalzik, K.J. Ebeling, J.-Ph. Poizat, Ph. Grangier, Opt. Lett. 24 (1999) 893.
[19] J.-P. Hermier, A. Branati, A.Z. Khoury, E. Giacobina, J.-Ph. Poizat, T.J. Chang, Ph. Grangier, J. Opt. Am. B 16 (1999) 2140.
[20] F. Prati, G. Fiacomelli, F. Marin, Phys. Rev. A 62 (2000) 33810.